© 2016. Published by The Company of Biologists Ltd | Development (2016) 143, 437-448 doi:10.1242/dev.133074

RESEARCH ARTICLE

Hoxb6 can interfere with somitogenesis in the posterior embryo through a mechanism independent of its rib-promoting activity

Ana Casaca, Ana Nóvoa and Moisés Mallo*

ABSTRACT

Formation of the vertebrate axial skeleton requires coordinated Hox gene activity. Hox group 6 genes are involved in the formation of the thoracic area owing to their unique rib-promoting properties. Here we show that the linker region (LR) connecting the homeodomain and the hexapeptide is essential for Hoxb6 rib-promoting activity in mice. The LR-defective Hoxb6 protein was still able to bind a target enhancer together with Pax3, producing a dominant-negative effect, indicating that the LR brings additional regulatory factors to target DNA elements. We also found an unexpected association between Hoxb6 and segmentation in the paraxial mesoderm. In particular, Hoxb6 can disturb somitogenesis and anterior-posterior somite patterning by dysregulation of *Lfng* expression. Interestingly, this interaction occurred differently in thoracic versus more caudal embryonic areas, indicating functional differences in somitogenesis before and after the trunk-to-tail transition. Our results suggest the requirement of precisely regulated *Hoxb6* expression for proper segmentation at tailbud stages.

KEY WORDS: Hox genes, Vertebrate patterning, Axial skeleton, Gene regulation, Mouse

INTRODUCTION

All vertebrates have an axial skeleton composed of individual vertebral units. Formation of the axial skeleton starts with the production of somites, which are epithelial blocks of paraxial mesoderm located on both sides of the developing neural tube (Brent and Tabin, 2002). Somites are formed sequentially in an anterior-to-posterior progression, coordinated with embryo growth at its posterior end. The process of somitogenesis involves the combined activity of a segmentation clock that sets the pace of somite formation and a moving front of tissue competence that determines the position of the posterior border of the next somite (Baker et al., 2006; Hubaud and Pourquié, 2014). The segmentation clock consists of waves of Notch, Fgf and Wnt signaling activities moving from the posterior to the anterior end of the presomitic mesoderm (PSM) (Dequéant et al., 2006; Hubaud and Pourquié, 2014). Notch signaling was the first pathway shown to have such oscillatory properties in the PSM (Palmeirim et al., 1997), and genetic studies have confirmed its central role in the segmentation process (Conlon et al., 1995; Oka et al., 1995; Saga et al., 1997; Wong et al., 1997; Evrard et al., 1998). Notch signaling promotes segmentation in the paraxial mesoderm. In the posterior PSM, however, this activity is silenced by inhibitory activities provided by Wnt and Fgf signaling (Hubaud and Pourquié, 2014) and Notch signaling activates instead a self-inhibitory feedback loop that generates the characteristic oscillations of this signaling pathway observed in this area. When a new cycle of Notch activity reaches an area of the anterior PSM containing Fgf and Wnt inhibitory activities below a threshold level, it triggers a molecular cascade that builds a new segment border, thus releasing a new somite at the anterior PSM margin (Baker et al., 2006; Hubaud and Pourquié, 2014). The cellular and molecular details of the segmentation process are still not fully understood, although some of the key regulators, including *Mesp2* and *Ripply2*, have already been identified (Morimoto et al., 2005, 2007; Oginuma et al., 2010).

Shortly after their formation, all somites are morphologically similar. However, they produce skeletal elements with unique anatomical features characteristic of their position along the anterior-posterior body axis. This regional differentiation of somites is to a large extent under the control of Hox genes (Pearson et al., 2005; Mallo et al., 2010; Casaca et al., 2014). In mammals, the Hox gene family is composed of 39 members distributed in four gene clusters resulting from two consecutive duplications of an ancestral cluster. As a consequence, each Hox gene within a particular cluster has close relatives in one or more of the other clusters with which they share the highest sequence similarity and relative position within the cluster. This led to the classification of Hox genes into 13 groups, normally known as paralog groups (PGs) (Prince, 2002; Duboule, 2007). A variety of genetic studies revealed that Hox proteins have a high degree of functional specificity, often shared by the different members of the same PG (Casaca et al., 2014). It is thought that morphological diversity in the axial skeleton results from the combined activities provided by the different Hox PGs (Mallo et al., 2009; Wellik, 2009).

Hox proteins of PGs 6 and 10 provide a paradigmatic example of how the coordinated activity of different Hox genes lays down major anatomical patterns in the axial skeleton (Wellik and Capecchi, 2003; Carapuço et al., 2005; McIntyre et al., 2007; Vinagre et al., 2010). Genes of both PGs regulate rib formation, but whereas Hox PG6 genes are able to promote this process, PG10 genes actively repress it. The sequential activity of PG6 and PG10 proteins as the embryo extends posteriorly results in the production of the cervical, thoracic and lumbar regions of the skeleton. Interestingly, both PG6 and PG10 proteins control rib formation at least in part by regulating an enhancer that controls *Myf5/6* expression in the hypaxial myotome (we refer to this as the H1 enhancer) (Vinagre et al., 2010). How Hox PG6 proteins activate and PG10 proteins repress this enhancer is only partially understood. However, biochemical and transgenic experiments indicate that the mechanisms used by the two Hox PGs are substantially different. In particular, Hoxb6 forms a complex with Pax3 to interact with the H1 enhancer and elicit hypaxial *Myf5/6* activation. The nature of this interaction is such that Hoxb6 is able to promote rib formation even when its intrinsic DNA-binding properties have been inactivated, as long as it can still interact

Instituto Gulbenkian de Ciência, Oeiras 2780-156, Portugal.

*Author for correspondence (mallo@igc.gulbenkian.pt)

Received 19 November 2015; Accepted 18 December 2015

Development (2016) 143, 437-448 doi:10.1242/dev.133074

with Pax3 (Guerreiro et al., 2013). Hoxa10, however, does not interact with Pax3 and its rib-blocking activity requires direct binding to the target enhancer (Guerreiro et al., 2013).

Hox proteins are transcription factors that bind DNA through their homeodomain (HD). It is clear that Hox functional specificity is largely encoded in non-HD parts of the protein (Zhao and Potter, 2001, 2002; Guerreiro et al., 2012), either in the form of intrinsic functional activities or by their ability to recruit additional factors (Mann et al., 2009; Casaca et al., 2014). Understanding the patterning activity of these Hox proteins thus requires the identification and characterization of the molecular signatures responsible for their functional specificity.

Here, we mapped the Hoxb6 protein to identify molecular signatures responsible for its rib-promoting properties. We show that the linker region (LR) connecting the HD and the hexapeptide (HX) motif is required but not sufficient for Hoxb6 rib-promoting activity in mice. The results of our transgenic and biochemical experiments suggest that Hoxb6/Pax3 binding to DNA serves as a docking complex to load additional factors into gene regulatory regions that control the transcriptional processes involved in rib induction. Our experiments also show that Hox gene activity can interfere with the segmentation clock. Interestingly, this interference seemed to occur differently at the thoracic versus more caudal areas of the skeleton, suggesting significant functional differences in the activity of the segmentation clock before and after the trunk-to-tail transition.

RESULTS

The linker region is important for Hox PG6 rib-promoting functions

To identify the molecular signatures providing rib-promoting activity to Hox PG6 proteins we compared the sequences of different members of this PG. Most sequence conservation was

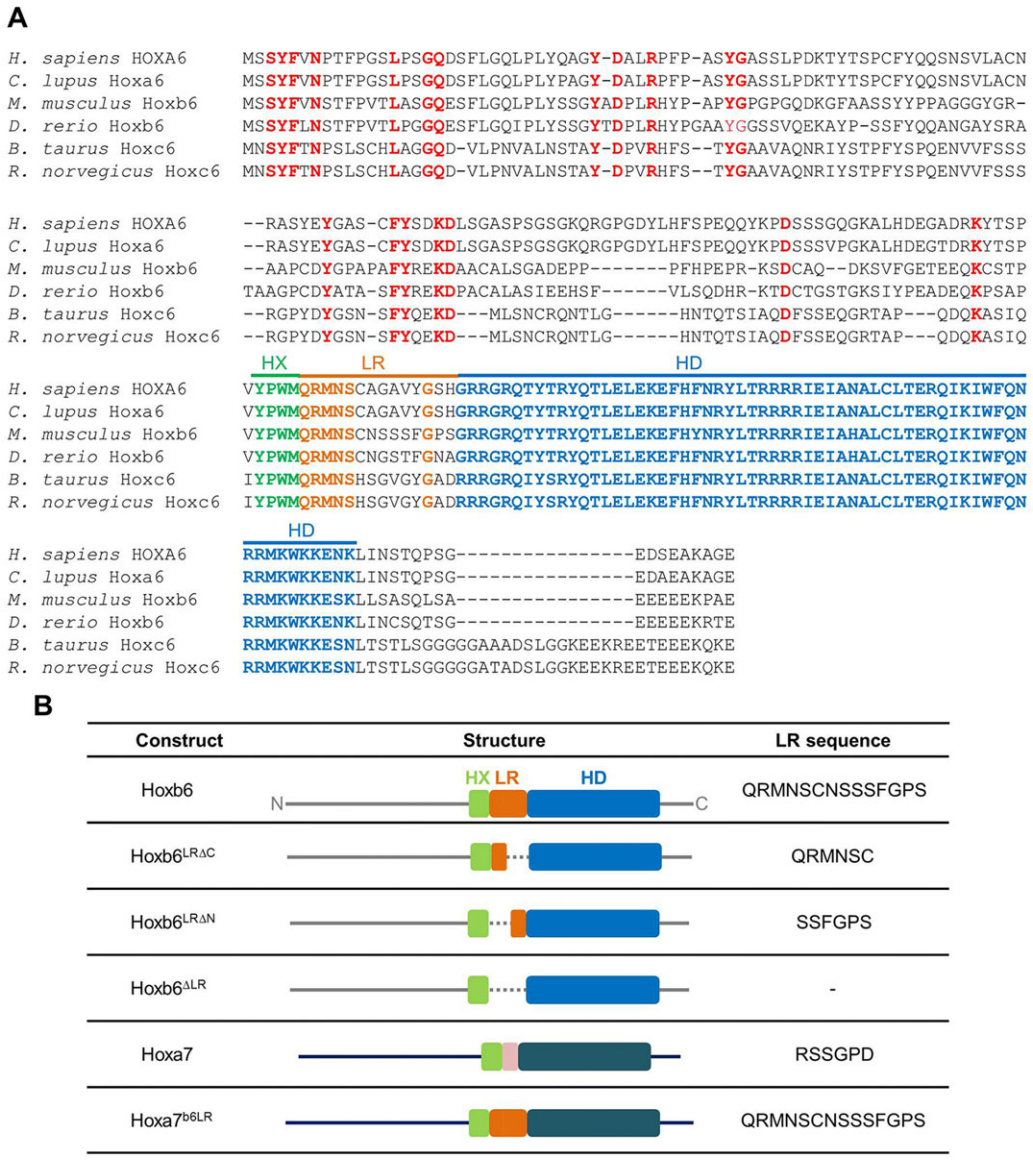

Fig. 1. Comparison of Hox PG6 protein sequences and the composition of constructs. (A) Alignment of protein sequences of Hox PG6 proteins of different vertebrates. The homeodomain (HD) is highlighted in blue and the hexapeptide (HX) in green. Identical amino acids in the linker region (LR) are highlighted in orange and identical amino acids outside these motifs are highlighted in red. (B) Hoxb6 and Hoxa7 constructs used in this work. HX, green; HD, light blue for Hoxb6, dark blue for Hoxa7; LR, orange for Hoxb6 and pink for Hoxa7; the remaining sequences are in gray for Hoxb6 and dark blue for Hoxa7. Dotted lines within constructs indicate deletions.

Development (2016) 143, 437-448 doi:10.1242/dev.133074

centered in and around the HD (Fig. 1, Fig. S1). Conserved motifs included the HX and the LR connecting the HX with the HD. All vertebrate Hox proteins of PGs 1 to 8 contain HX sequences (In der Rieden et al., 2004) and it is therefore unlikely that this motif is the source of Hox PG6 functional specificity. The LR, however, shows Hox PG6-specific features. These include its length (14 amino acids) (Sharkey et al., 1997; In der Rieden et al., 2004) and strong sequence conservation at the N-terminal half (QRMNSC) (Fig. 1). Work performed mainly in *Drosophila* showed that Hox LRs are not simple inert spacers but that they contribute actively to the functional properties of Hox proteins (Gebelein et al., 2002; Merabet et al., 2003; Joshi et al., 2010; Reed et al., 2010; Papadopoulos et al., 2011). Therefore, we focused our analysis on this area of the Hoxb6 protein.

We created *Hoxb6* deletion mutants and tested their rib-inducing activity in transgenic mice. To examine whether LR length was itself important for Hoxb6 functional properties we first produced mutant versions of Hoxb6 containing six-amino-acid LRs, thus mimicking its length in Hox PG7 proteins (Fig. 1), which lack rib-inducing properties (Table 1). The activity of the mutant Hoxb6 proteins varied depending on whether the deletion removed the C-side or N-side of the LR (Hoxb6$^{LR\Delta C}$ and Hoxb6$^{LR\Delta N}$, respectively). In particular, Hoxb6$^{LR\Delta C}$ (LR of sequence QRMNSC) not only retained full rib-promoting properties, but seemed even more active than the native Hoxb6. This idea was based on the fact that a higher proportion of *Dll1-Hoxb6*$^{LR\Delta C}$ transgenics showed a phenotype than *Dll1-Hoxb6* (although with the numbers analyzed this was not statistically significant; Table 1), and on the observation that in *Dll1-Hoxb6*$^{LR\Delta C}$ transgenic embryos ectopic ribs seemed longer and often associated with a greater number of vertebral segments than in transgenics expressing *Hoxb6* (Fig. 2A). Conversely, removal of the N-side of the LR (LR of sequence SSFGPS) compromised Hoxb6 rib-inducing capacity, as we could not find any *Dll1-Hoxb6*$^{LR\Delta N}$ transgenic embryos displaying a complete 'all-rib' phenotype. We observed ectopic ribs in five out of the eight specimens analyzed, but they never covered as much of the body axis as in transgenics expressing Hoxb6$^{LR\Delta C}$ or Hoxb6 (Table 1 and Fig. 2A).

We next analyzed whether the LR is required for the rib-promoting properties by creating a mutant Hoxb6 lacking this region (Hoxb6$^{\Delta LR}$). None of the *Dll1-Hoxb6*$^{\Delta LR}$ transgenic embryos analyzed contained extra ribs (Table 1). On the contrary, they had rib deficiencies affecting the first and last thoracic segments (Fig. 2Ae,j,o), resembling a *Hoxb6* loss-of-function phenotype (McIntyre et al., 2007).

Altogether, these data indicate that the LR is required for Hoxb6 rib-promoting function and that this property is unlikely to be dependent on its length but rather on specific properties of its amino acid sequence. Also, the observation that alterations in the LR can lead to increased or decreased Hoxb6 functional activity, depending on the remaining sequence, suggests the existence of functional interactions between different parts of the LR.

To determine whether the Hoxb6 LR is sufficient to provide Hox proteins with rib-inducing activity we substituted the LR sequence of Hoxa7, which lacks rib-inducing properties in our transgenic assay, with the LR of Hoxb6 (Hoxa7^{B6LR}). All *Dll1-Hoxa7*^{B6LR} transgenic fetuses recovered at embryonic day (E) 18.5 had normal-looking axial skeletons (Table 1), indicating that the LR of Hoxb6 is not sufficient to confer rib-promoting properties to other Hox proteins. This suggests that the rib-inducing properties of Hoxb6 require the presence of additional characteristics that are specific to this protein.

Table 1. Summary of the transgenics analyzed and their distribution according to the type of phenotype obtained

Construct	Transgenics analyzed	Type of phenotype			
		I	II	III	IV
Hoxb6$^{LR\Delta C}$	13	3	0	0	5
Hoxb6$^{LR\Delta N}$	9	0	5	0	4
Hoxb6$^{\Delta LR}$	15	0	0	3	5
Hoxa7	5	0	0	0	0
Hoxa7^{B6LR}	11	0	0	0	0
Hoxb6^{ShortUTR}	26	2	8	0	9
Hoxb6^{LongUTR}	21	6	5	0	6
Hoxb6$^{LR\Delta C_LongUTR}$	13	1	2	0	3

Type I: specimens showing an 'all-rib' phenotype, with ribs in vertebral segments from the cervical to the caudal area. Type II: specimens showing intermediate rib phenotypes, exhibiting rudimentary ribs in the cervical, lumbar and/or sacral region. Type III: specimens lacking ribs unilaterally or bilaterally in the first and/or second thoracic vertebrae. Type IV: specimens showing posterior segmentation defects starting at the level of the thoracic/lumbar transitions in the more affected transgenics. Transgenic embryos analyzed but not listed under Types 1-4 were indistinguishable from wild type in phenotype.

Hoxb6 DNA-binding capacity is independent of the LR

We have recently shown that in the mouse Hoxb6 rib-promoting activity relies on its binding to the H1 enhancer of the *Myf5/6* genes in a complex with Pax3 (Vinagre et al., 2010; Guerreiro et al., 2013). We tested whether alterations in the LR could influence Hoxb6 interactions with Pax3 and/or with the *Myf5/6* H1 enhancer using an electrophoretic mobility shift assay. Comparison of the patterns obtained with the different versions of Hoxb6 revealed no fundamental changes in their capacity to bind the H1 enhancer either alone or in a complex with Pax3 (Fig. 2B). Remarkably, even Hoxb6$^{\Delta LR}$, which completely lacked rib-inducing activity, was able to bind H1 in a complex with Pax3. Together, these results indicate that the different activities of the various Hoxb6 LR mutant proteins are not related to their differential ability to bind the H1 enhancer.

Interestingly, neither Hoxa7 nor Hoxa7^{B6LR} seemed to interact with the H1 enhancer as a complex with Pax3 (Fig. 2C). This suggests that although the Hoxb6 LR is not involved in the formation of the Hox-Pax3-H1 enhancer complex, it can only trigger activity when the Hox protein is bound to the H1 enhancer as a complex with Pax3.

Segmentation defects are associated with all Hoxb6 mutant proteins

In the course of the previous experiments we observed that some transgenic embryos had vertebral malformations, including a variety of vertebral fusions and highly disorganized vertebrae. In some cases this led to posterior body truncations affecting the lumbar and more posterior axial structures (Fig. 3A and Table 1). Cervical vertebrae were also affected, although malformations in this area were milder than those observed in posterior anatomical regions (Fig. 3). In previous experiments involving *Dll1-Hoxb6* we had found one case with an equivalent phenotype. Its isolated nature had led us to consider it as an indirect consequence of the transgene insertion site. However, the vertebral malformations that we now observed were present in a considerable number of transgenics and were associated with all mutant versions of Hoxb6. This ruled out positional effects and indicated that they resulted from Hoxb6 activity.

Development (2016) 143, 437-448 doi:10.1242/dev.133074

The cloning strategy used to produce the constructs of the present work resulted in the removal of the last 480 bp of the *Hoxb6* 3′UTR (Fig. 3B), which were included in the construct used in our initial experiments expressing the wild-type Hoxb6 (Vinagre et al., 2010). To determine whether the apparent lack of vertebral malformations in *Dll1-Hoxb6* transgenics was related to intrinsic properties of wild-type Hoxb6 or to the presence of the complete 3′UTR we generated transgenics with a construct containing the wild-type Hoxb6 sequence and the incomplete 3′UTR (*Hoxb6*^{ShortUTR}). We detected vertebral malformations in *Dll1-Hoxb6*^{ShortUTR} transgenics (Fig. 3Ae,k), indicating that native Hoxb6 can induce the same types of vertebral phenotype as the mutant proteins. We also created additional *Dll1-Hoxb6*^{LongUTR} transgenics. Six out of 21 of these transgenics showed segmentation defects (Table 1), a lower penetrance than that observed with *Dll1-Hoxb6*^{ShortUTR}. This result suggests that the 3′UTR can influence Hoxb6 activity, a subject that will be further explored below.

Segmentation defects were found in transgenics expressing all variants of Hoxb6, regardless of their ability to induce rib formation. However, the penetrance and severity of the vertebral malformations varied among the different Hoxb6 versions, roughly correlating with the strength of their rib phenotypes. These results thus seem to indicate that although the ability of Hoxb6 to interfere with the segmentation process is apparently independent of its rib-promoting properties, both activities might somehow be linked.

Establishment and characterization of *Dll1-Hoxb6*$^{\Delta LR}$ transgenic lines

To overcome the phenotypic variability inherent to transient microinjections we tried to produce transgenic lines for the different versions of Hoxb6. We were unable to produce stable lines for *Dll1-Hoxb6* and *Dll1-Hoxb6*$^{LR\Delta C}$ despite repeated attempts, as transgenics for these constructs consistently died within the first postnatal hours. We were more successful with the *Dll1-Hoxb6*$^{\Delta LR}$ construct, as we obtained two viable transgenic males (*Dll1-Hoxb6*$^{\Delta LR}$*_1* and *Dll1-Hoxb6*$^{\Delta LR}$*_2*). Both transgenic mice showed kinked tails and a reduction in tail and body length, although the severity of the phenotype differed between the two animals. We could not establish stable lines from any of these two founders as the transgenic progeny

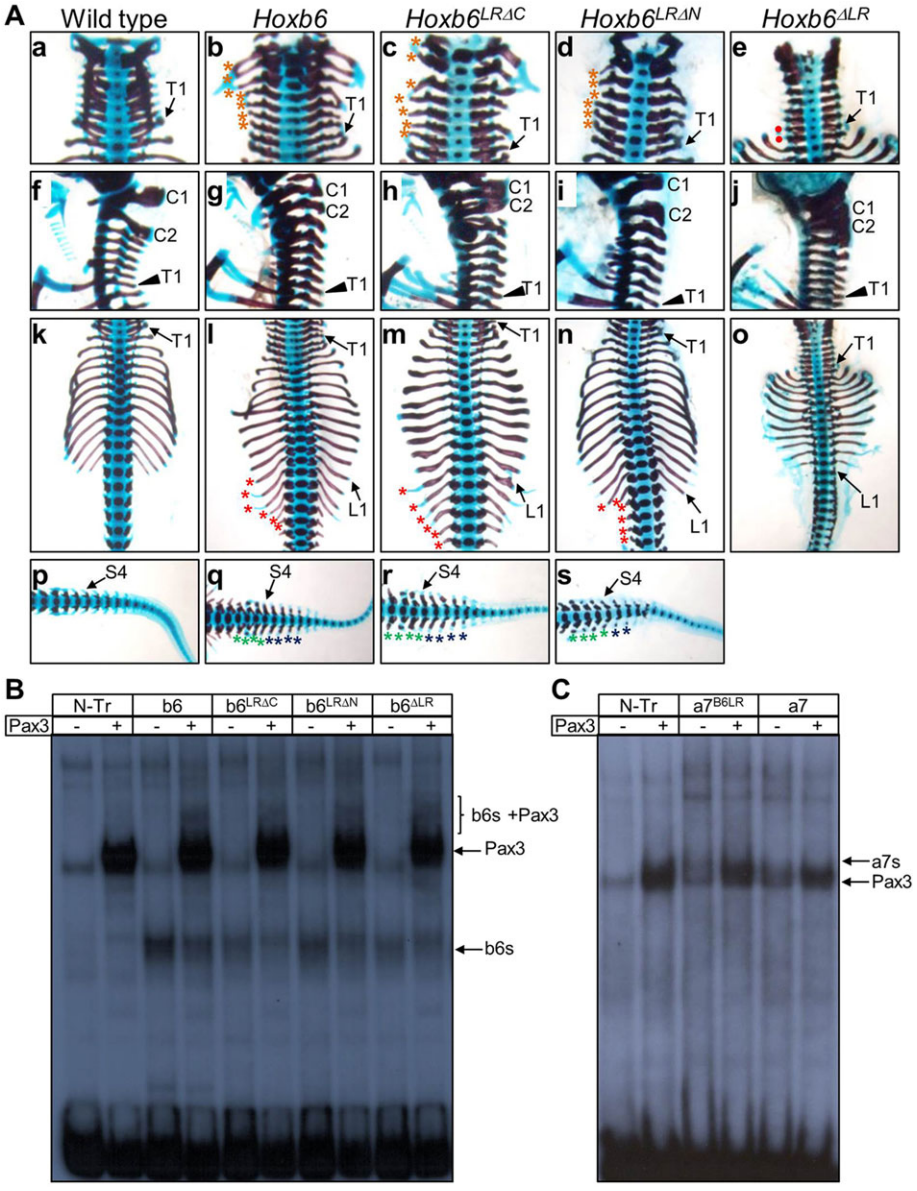

Fig. 2. Rib phenotypes of transgenic mice expressing various versions of the Hoxb6 protein and their DNA-binding activities. (A) Dorsal views of cervical (a-e), thoracic to lumbar (k-o) and sacral to caudal (p-s) areas of the skeleton and lateral views of the cervical region (f-j) of wild-type (a,f,k,p), *Dll1-Hoxb6* (b,g,l,q), *Dll1-Hoxb6*$^{LR\Delta C}$ (c,h,m,r), *Dll1-Hoxb6*$^{LR\Delta N}$ (d,i,n,s) and *Dll1-Hoxb6*$^{\Delta LR}$ (e,j,o) E18.5 fetuses. The first cervical vertebrae (C1 and C2), the first thoracic (T1), the first lumbar (L1) and the fourth sacral (S4) vertebra are indicated. Asterisks indicate extra ribs in the cervical (orange), lumbar (red), sacral (green) and caudal (dark blue) regions. Red circles indicate the absence of ribs in the thoracic region. (B,C) Electrophoretic mobility shift assay using a probe of the *Myf5* H1 enhancer and different versions of the Hoxb6 (B) or Hoxa7 (C) and Pax3 proteins, showing the patterns obtained with non-transfected extracts (N-Tr), Hoxb6, Hoxb6$^{LR\Delta C}$, Hoxb6$^{LR\Delta N}$, Hoxb6$^{\Delta LR}$, Hoxa7^{B6LR} and Hoxa7 alone or together with Pax3. Arrows indicate the position of complexes with the different versions of Hoxb6 (b6s), Pax3 or the different versions of Hoxa7 (a7s) proteins. Bracket indicates Hoxb6-Pax3-H1 complexes.

Development (2016) 143, 437-448 doi:10.1242/dev.133074

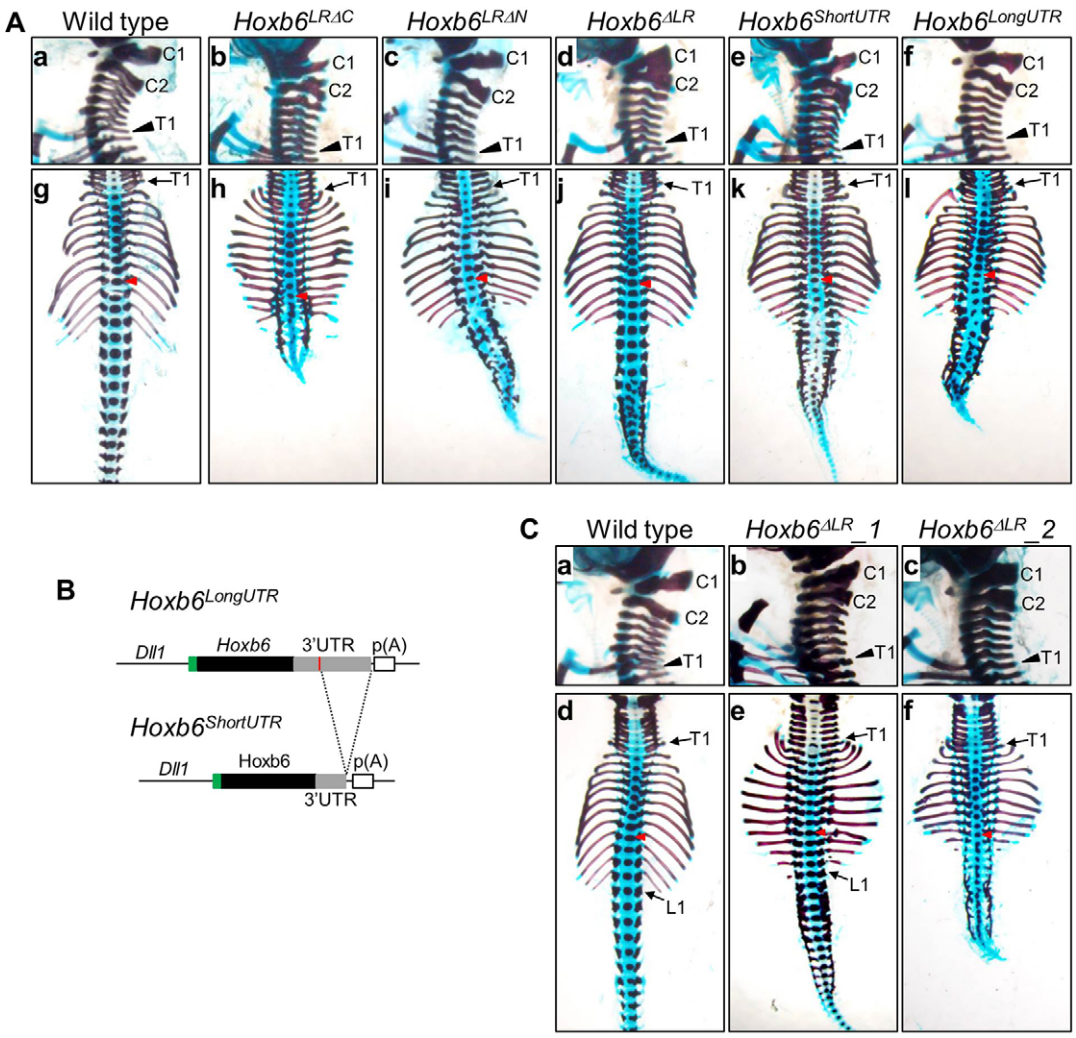

Fig. 3. Segmentation phenotypes of transgenic mice expressing different versions of the Hoxb6 protein. (A) Skeletal analysis showing lateral views of cervical areas (a-f) and dorsal views of thoracic to caudal areas (g-l) of wild-type (a,g), *Dll1-Hoxb6*$^{LR\Delta C}$ (b,h), *Dll1-Hoxb6*$^{LR\Delta N}$ (c,i), *Dll1-Hoxb6*$^{\Delta LR}$ (d,j), *Dll1-Hoxb6*^{ShortUTR} (e,k) and *Dll1-Hoxb6*^{LongUTR} (f,l) fetuses at E18.5. (B) *Hoxb6* transgenes containing the long or short versions of the 3′UTR. The Flag tag (green rectangle) and the SV40 polyadenylation signal p(A) are shown. The red line marks the *Xho*I site in the 3′UTR of human *HOXB6* mRNA used in the cloning strategy. (C) Skeletal analysis showing lateral views of cervical areas (a-c) and dorsal views of thoracic to caudal areas (d-f) of wild-type (a,d), *Dll1-Hoxb6*$^{\Delta LR}$*_1* (b,e) and *Dll1-Hoxb6*$^{\Delta LR}$*_2* (c,f) E18.5 fetuses. The first cervical (C1 and C2), the first thoracic (T1), the first lumbar (L1) and the tenth thoracic (red arrowhead) vertebrae are indicated.

died immediately after birth, exhibiting severe malformations in the axial skeleton, suggesting that these two founders were most likely chimeras. Still, the two founder males bred well and transmitted the transgene to the offspring, thus allowing a more detailed analysis of their phenotypes at different stages of development.

Transgenic embryos from founders *Dll1-Hoxb6*$^{\Delta LR}$*_1* and *Dll1-Hoxb6*$^{\Delta LR}$*_2* had skeletal characteristics consistent with those described for the transient transgenics obtained with this construct (Fig. 2Ae,j,o and Fig. 3Cb,c,e,f). The specific skeletal patterns were consistent within the transgenic line (n=3 and n=4 for *Dll1-Hoxb6*$^{\Delta LR}$*_1* and *Dll1-Hoxb6*$^{\Delta LR}$*_2*, respectively), but malformations were stronger in fetuses from line number 2. Disruption of segmental patterns was clear at the end of the thoracic region of *Dll1-Hoxb6*$^{\Delta LR}$*_2* embryos, with the appearance of malformed vertebral bodies and fusions of adjacent neural arches. The cervical region was also affected mainly in C1 and C2, showing thicker neural arches that were occasionally fused. The remaining cervical vertebrae were also affected, showing abnormal morphologies and reduced intervertebral spaces (Fig. 3Cc). We therefore mostly used embryos from the *Dll1-Hoxb6*$^{\Delta LR}$*_2* line for the analyses at earlier stages.

Molecular analysis of segmentation phenotypes

To understand the mechanism that originated the vertebral deficiencies in *Hoxb6*-expressing transgenics, we performed a molecular analysis at E10.5. For these experiments, in addition to embryos from the *Dll1-Hoxb6*$^{\Delta LR}$*_2* line we also used transient *Dll1-Hoxb6*$^{LR\Delta C}$ transgenics because they had visible morphological alterations in the posterior somites that allowed the identification of transgenic embryos during dissection.

Paraxis (*Tcf15* – Mouse Genome Informatics) expression revealed that *Dll1-Hoxb6*$^{LR\Delta C}$ embryos failed to form individual segments in the paraxial mesoderm (Fig. 4A-D). Interestingly, this segmentation phenotype was restricted to posterior somites, starting around somite 24. Somites anterior to this level,

Development (2016) 143, 437-448 doi:10.1242/dev.133074

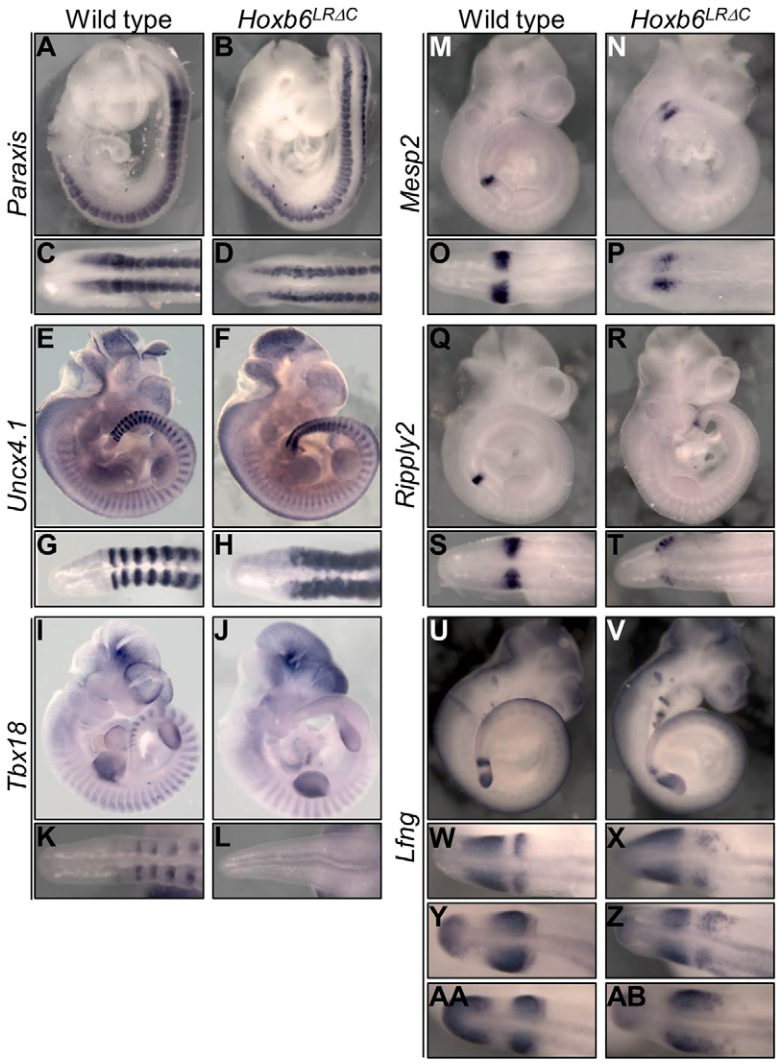

Fig. 4. Late somitogenesis is not perturbed in *Dll1-Hoxb6*$^{LR\Delta C}$ embryos. Wild-type and *Dll1-Hoxb6*$^{LR\Delta C}$ transgenic embryos were analyzed at E10.5 for the molecular markers *Paraxis* (A-D), *Uncx4.1* (E-H), *Tbx18* (I-L), *Mesp2* (M-P) and *Ripply2* (Q-T). *Lfng* expression (U-AB) is shown in three different wild-type and transgenic embryos to show the different stages of oscillatory expression in the PSM.

however, seemed to have formed properly. Similar features were observed in *Dll1-Hoxb6*$^{\Delta LR}$*_2* embryos (Fig. 5A-D). We also analyzed anterior-posterior somite patterning using *Uncx4.1* and *Tbx18* expression, which mark posterior and anterior somite halves, respectively (Neidhardt et al., 1997; Bussen et al., 2004). At E10.5 both *Uncx4.1* (*Uncx* – Mouse Genome Informatics) and *Tbx18* expression followed normal patterns in somites anterior to the hindlimb in *Dll1-Hoxb6*$^{LR\Delta C}$ and *Dll1-Hoxb6*$^{\Delta LR}$*_2* transgenic embryos (Fig. 4E-L and Fig. 5E-L). However, posterior to somite 24, *Uncx4.1* expression was expanded following a pattern resembling that of *Paraxis*, and *Tbx18* expression was mostly lost. These results indicate that the paraxial mesoderm posterior to the hindlimb has not only failed to undergo segmentation but also lacked proper anterior-posterior patterning, acquiring posterior-like identity.

We then analyzed *Lfng* expression as a readout of the segmentation clock. At E10.5 we found transgenic embryos for both *Dll1-Hoxb6*$^{LR\Delta C}$ and *Dll1-Hoxb6*$^{\Delta LR}$*_2* in different phases of the cycle (Fig. 4U-AB and Fig. 5U-AB). We were also unable to detect alterations in the expression of the cycling gene *Hes7* in *Dll1-Hoxb6*$^{\Delta LR}$*_2* (Fig. 5AC-AH), indicating that the segmentation clock remained mostly undisrupted. However, the *Lfng* signal in the anterior PSM was clearly affected in all embryos analyzed, regardless of its expression in the posterior PSM (Fig. 4U-AB and Fig. 5U-AB). In particular, it had lost its characteristic sharpness, spreading along the anterior-posterior axis in a salt-and-pepper pattern. Expression of *Mesp2* and *Ripply2* was also altered in both transgenics, following patterns resembling those observed for *Lfng* in the anterior PSM, including an extended expression domain in the anterior-posterior axis and a salt-and-pepper distribution of the transcripts (Fig. 4M-T and Fig. 5M-T).

Dll1-Hoxb6$^{\Delta LR}$*_2* embryos had patterning defects in the cervical domain in addition to the malformations in the lumbo-sacral region. Expression analysis of *Paraxis* and *Uncx4.1* at E8.5 (when the cervical region is being laid down) revealed patterns indistinguishable from those observed in wild-type embryos (Fig. 6A-D), indicating that the phenotypic alterations observed at cervical and lumbo-sacral levels of transgenic embryos were produced through different mechanisms. In this area we also took a closer look at *Hes7* expression, as alterations in the expression of this gene [pH7-Hes7-3 mice in Harima et al. (2013)] produced phenotypes in the cervical region resembling those observed in *Dll1-Hoxb6*$^{\Delta LR}$ transgenics. In our analyses we could not detect any obvious deviation from the normal *Hes7* expression patterns (Fig. 6K-P), although we cannot rule out the existence of more subtle changes that escaped detection by regular *in situ* hybridization analyses. We also failed to find alterations in *Lfng* expression at E8.5 (Fig. 6E-J). Together, these results indicate that

Development (2016) 143, 437-448 doi:10.1242/dev.133074

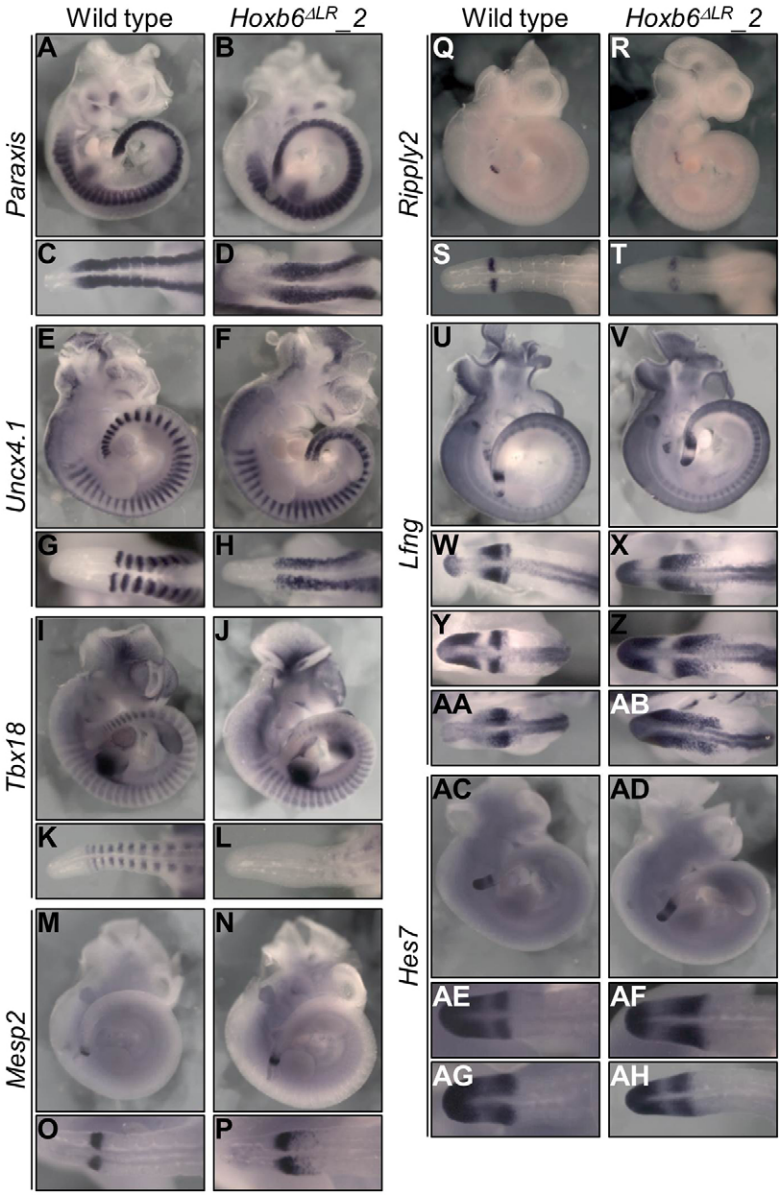

Fig. 5. Late somitogenesis is not perturbed in *Dll1-Hoxb6*$^{\Delta LR}$ embryos. Wild-type and *Dll1-Hoxb6*$^{\Delta LR}$*_2* embryos were analyzed at E10.5 for the molecular markers *Paraxis* (A-D), *Uncx4.1* (E-H), *Tbx18* (I-L), *Mesp2* (M-P) and *Ripply2* (Q-T). *Lfng* expression (U-AB) is shown in three different wild-type and transgenic embryos to show different stages of oscillatory expression in the PSM. *Hes7* expression (AC-AH) is shown in the PSM of two wild-type and two *Dll1-Hoxb6*$^{\Delta LR}$*_2* embryos corresponding to two different phases of the expression cycle.

Hoxb6 activity affects somitogenesis differently in the anterior and posterior embryonic domains.

Hoxb6 expression levels and phenotypic outcome

An interesting aspect of the segmentation phenotypes of transgenics expressing Hoxb6 proteins was that malformations were more striking in axial regions posterior to the thorax. To investigate whether this was related to different levels of transgenic *Hoxb6* transcription at the various axial levels we assessed transgene expression in embryos of the *Dll1-Hoxb6*$^{\Delta LR}$*_1* and *Dll1-Hoxb6*$^{\Delta LR}$*_2* lines from E8.5 to E10.5 to cover stages corresponding to the formation of different levels of the main body axis. The probe used for these experiments detects both endogenous and transgene-derived *Hoxb6* mRNAs. Therefore, to evaluate the possible contribution of the endogenous *Hoxb6* transcripts to the image obtained with the transgenics we also analyzed wild-type embryos at the same stage. Embryos from both founders showed similar expression patterns, consisting in strong *Hoxb6* expression in the PSM (Fig. 7G-L), at all stages analyzed. The absence of any obvious stage-related differences in *Hoxb6* expression in the PSM of these transgenics indicates that the differential regional distribution of the segmentation malformations did not derive from region-specific variations in transgene expression. Also, direct comparison of *Hoxb6* expression in the two transgenic lines indicated higher expression levels in *Dll1-Hoxb6*$^{\Delta LR}$*_2* than in *Dll1-Hoxb6*$^{\Delta LR}$*_1*, suggesting that the different severities of their skeletal phenotypes derived from expression levels.

In contrast to the uniform distribution of *Hoxb6* transcripts in the transgenics, endogenous *Hoxb6* gene expression was clearly regionalized. As previously described (Becker et al., 1996), *Hoxb6* expression started around E8.5, when it was detected as a weak signal in the PSM (Fig. 7A). Higher *Hoxb6* expression levels were observed at E9.5 in the paraxial mesoderm, including both the presomitic and somitic mesoderm, with an anterior expression border at somite 12 (Fig. 7B). At E10.5 endogenous *Hoxb6* expression in the somitic mesoderm retained the anterior boundary but became downregulated in more posterior areas (starting around somite 24). At this stage the PSM was clearly negative for *Hoxb6* expression (Fig. 7C,F,F′

Development (2016) 143, 437-448 doi:10.1242/dev.133074

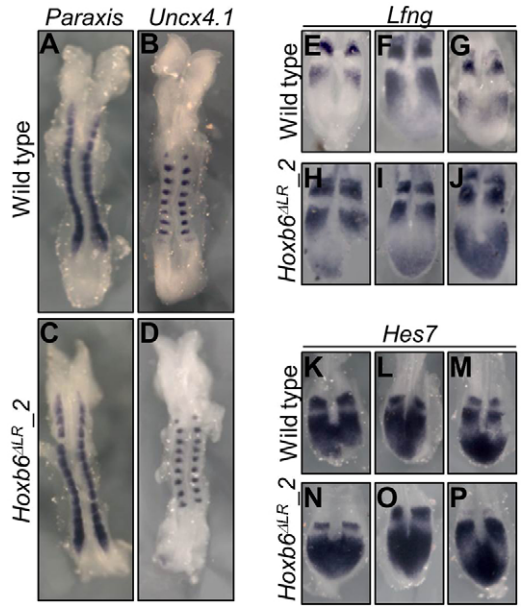

Fig. 6. Early somitogenesis is not perturbed in *Dll1-Hoxb6*$^{\Delta LR}$ embryos. Wild-type (A,B,E-G,K-M) and *Dll1-Hoxb6*$^{\Delta LR}$*_2* transgenic (C,D,H-J,N-P) embryos were analyzed for molecular markers at E8.5. Comparison of expression of *Paraxis* (A,C) and *Uncx4.1* (B,D) showed no differences between wild type and transgenics. There were no obvious differences in the oscillatory expression of *Lfng* (E-J) and *Hes7* (K-P) in transgenic embryos when compared with wild type.

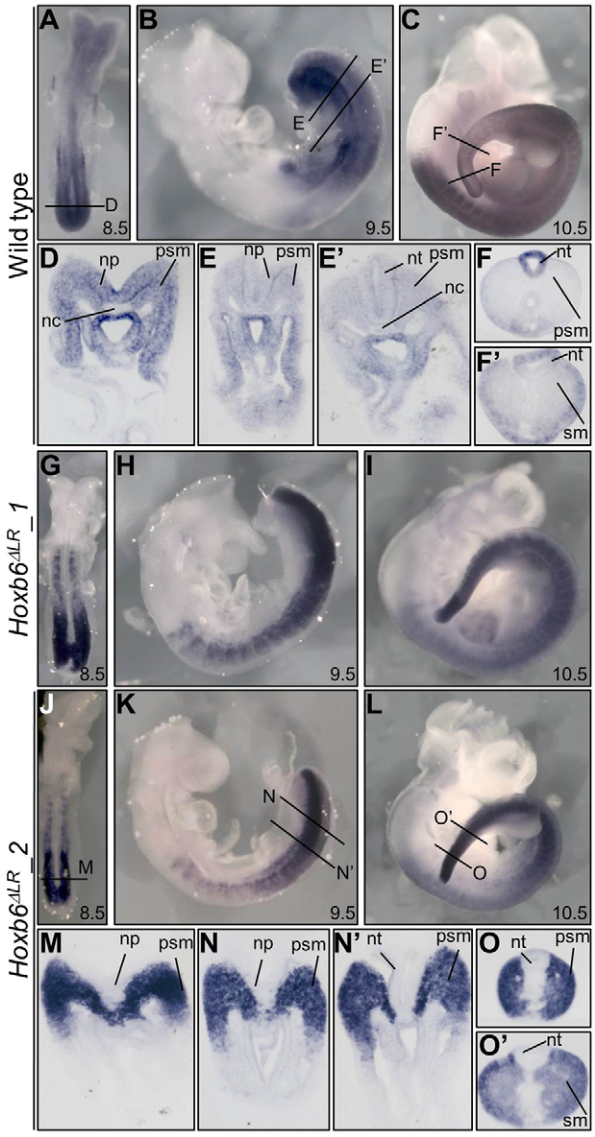

Fig. 7. Expression of *Hoxb6* in wild-type and *Dll1-Hoxb6*$^{\Delta LR}$ embryos. Whole-mount *in situ* hybridization at E8.5 (A,G,J), E9.5 (B,H,K) and E10.5 (C,I,L), and transverse vibratome sections (D-F′,M-O′) at the levels indicated by the lines. Wild-type (A-C) and transgenic (G-I, *Dll1-Hoxb6*$^{\Delta LR}$*_1*; J-L, *Dll1-Hoxb6*$^{\Delta LR}$*_2*) embryos are shown. Note that development of the color reaction was more rapid in the transgenic than in the wild-type embryos. nc, notochord; np, neural plate; psm, presomitic mesoderm; nt, neural tube; sm, somites.

and Fig. 8C). This contrasted with the strong *Hoxb6* expression seen in the PSM of similarly staged transgenic embryos (Fig. 7J-O′).

Analysis of these expression patterns in the context of the segmentation phenotypes of *Hoxb6* transgenics indicates that the PSM corresponding to axial levels that in wild-type embryos express *Hoxb6* (eventually giving rise to the thoracic area) seemed to be more permissive to high *Hoxb6* dosages than the PSM corresponding to areas that normally develop in the absence of *Hoxb6*. In addition, these observations suggest that the physiological *Hoxb6* downregulation occurring in the PSM that generates the posterior skeleton might be required for the normal development of lumbar, sacral and caudal vertebrae.

miR196 and miR199 do not appear to play a role in *Hoxb6* regulation

The strength of the phenotypes observed in *Dll1-Hoxb6* transgenic embryos depended on the extent of the 3′UTR included in the construct. Similar experiments performed with Hoxb6$^{LR\Delta C}$ pointed to the same conclusion, although with the number of embryos analyzed the difference was not statistically significant (Table 1). These observations suggested that the last 480 nucleotides of the 3′UTR might include some element affecting either mRNA production or stability. We therefore explored whether this region of the 3′UTR might be responsible for the absence of *Hoxb6* transcripts in the PSM forming vertebral elements caudal to the thorax.

Central Hox genes have been shown to be under the regulation of microRNAs (miRs) (Yekta et al., 2008). Therefore, we searched for miR targets in this area of the *Hoxb6* 3′UTR. A bioinformatic analysis revealed the presence of several miR binding sites, most of which were conserved between mouse and human (Fig. 8A,B, Fig. S2). These included miR196, which is known to be involved in the regulation of several Hox genes (Yekta et al., 2004, 2008). In addition, deletion of the three miR196 family members produced alterations in the identity and/or number of vertebrae in the mouse (Wong et al., 2015). This area of the *Hoxb6* 3′UTR also contains a target for miR199, mutants of which display skeletal defects (Watanabe et al., 2008). To test whether these miRs are involved in the regulation of *Hoxb6* expression we created mutant mice (*Hoxb6*$^{\Delta 3'UTR412\text{-}435}$) lacking these sites in the *Hoxb6* 3′UTR using CRISPR/Cas9 technology. The deleted region also includes the seed regions of miR145 and miR185 (Fig. 8A,B). Mice homozygous for this deletion were apparently normal, fertile and had no skeletal abnormality. *Hoxb6* expression in these mutants also resembled wild-type patterns (Fig. 8C). Therefore, miR196 and miR199 (as well as miR185 and miR145) do not seem to play any essential role in the regulation of *Hoxb6* expression in the posterior embryo.

Development (2016) 143, 437-448 doi:10.1242/dev.133074

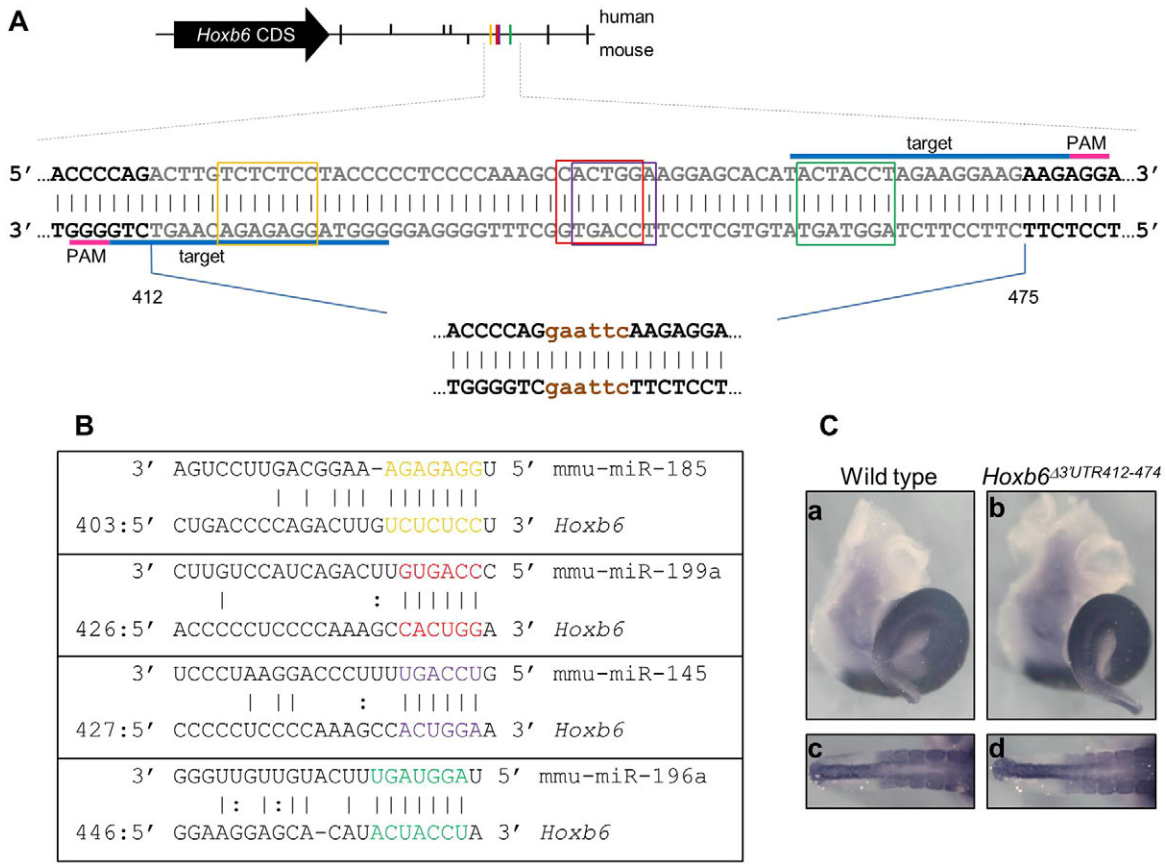

Fig. 8. miR196 and miR199 do not appear to regulate *Hoxb6* expression. (A) Position of predicted miR binding sites in the human and mouse *Hoxb6* 3′UTRs according to TargetScan and/or microRNA.org tools. From left to right, the human 3′UTR contains targets for miR211/202, miR873, miR494, miR335 (all in black), miR185 (yellow), miR199a (red), miR145 (purple), miR 196a/b (green), miR376c and miR23a/b (both in black) and the mouse sequence contains targets for miR211/202, miR370 (both in black), miR185 (yellow), miR199a (red), miR145 (purple), miR196a/b (green), miR376c and miR23a/b (both in black). A zoom in of the region deleted in the *Hoxb6*$^{\Delta 3'UTR412\text{-}474}$ mutant embryos is also shown indicating the sites using the same color code. The sequence after deletion is shown beneath, which introduced an *Eco*RI site (orange). The 20 bp targets recognized by the sgRNAs are highlighted in blue and the protospacer adjacent motif (PAM) sequences in pink. CDS, coding sequence. (B) Alignments between miRs and mouse *Hoxb6* 3′UTR sequence predicted with TargetScan or microRNA.org tools. (C) Whole-mount *in situ* hybridization showing no differences in *Hoxb6* expression between wild-type (a,c) and *Hoxb6*$^{\Delta 3'UTR412\text{-}474}$ mutant (b,d) embryos.

DISCUSSION

Hox PG6 proteins are unique in their ability to promote rib formation and this function is crucial for the formation of the thoracic area (McIntyre et al., 2007; Vinagre et al., 2010). Here, we showed that although the LR is essential for the rib-promoting activity of Hoxb6, it is not sufficient to endow other Hox proteins with a similar functional property. We have previously shown that Hoxb6 builds a functional complex with Pax3 to activate the H1 enhancer of *Myf5/6* (Vinagre et al., 2010; Guerreiro et al., 2013) as part of its rib-promoting mechanism. Therefore, the Hoxb6 LR could be the region linking Hoxb6 and Pax3. This hypothesis is however very unlikely because Hoxb6$^{\Delta LR}$ was still able to form a Pax3-Hoxb6 complex with the H1 enhancer in an *in vitro* assay, and Hoxa7 did not form a complex with Pax3 on the H1 enhancer even when it contained the Hoxb6 LR. An alternative possibility is that the LR recruits additional factors required to activate functional properties of the Hoxb6-Pax3 complex when bound to the H1 enhancer. This hypothesis provides a suitable explanation for the rather surprising observation that the LR-defective Hoxb6 protein did not simply lose its rib-promoting activity but instead produced a phenotype resembling that of a *Hoxb6* loss of function (McIntyre et al., 2007), suggesting that Hoxb6$^{\Delta LR}$ could act as a dominant-negative version of Hoxb6. Accordingly, Hoxb6$^{\Delta LR}$-Pax3 binding to the H1 enhancer would not only be non-productive but also, when in excess, might block access of the endogenous Hoxb6 protein to the regulatory region. In this scenario, the inability of Hoxa7^{B6LR} to promote rib formation would derive from its failure to form a complex with Pax3 at the H1 enhancer.

Our data indicate that the LR is required to provide specific activities to the Hoxb6 protein. However, the length of the LR, despite being one of the defining features of Hox PG1 to 8 proteins (Sharkey et al., 1997; In der Rieden et al., 2004), plays little role in providing functional specificity. Instead, it seems that the amino acid composition of the LR could be one of the key factors relevant for its function. Interestingly, the differences in apparent activity provided by the residues next to the HX or to the HD suggest that the regions either side of the LR make distinct contributions and that regulatory interactions among these regions are required to properly control protein activity. Understanding these interactions and how they trigger Hoxb6 functional activity will require the identification and characterization of the factors that interact with this region of the protein.

Hoxb6 can interfere with the segmentation program

An unexpected finding of our work is that forced *Hoxb6* expression in the paraxial mesoderm also produced non-rib-

Development (2016) 143, 437-448 doi:10.1242/dev.133074

related malformations in the axial skeleton. These phenotypes were qualitatively different at the various levels of the anterior-posterior embryonic axis. In the neck the alterations comprised identity changes affecting the anterior cervical vertebrae, which in the strongest cases could be scored as a duplication of the atlas. Intriguingly, this phenotype is remarkably similar to that described for pH7-Hes7-3 mice in which *Hes7* expression in the PSM oscillates more rapidly than in wild-type embryos (Harima et al., 2013), suggesting that Hox genes might be involved in tuning the oscillatory behavior of *Hes7*. Our analysis of *Hes7* expression in *Dll1-Hoxb6*$^{\Delta LR}$ transgenic embryos was not sensitive enough to properly evaluate this hypothesis and, therefore, it is currently not possible to decide on the existence of a Hox-*Hes7* connection. However, additional observations make this potential Hox-*Hes7* connection worth exploring. In particular, it has been described that *Hoxd1* and *Hoxd3* display oscillatory expression in the PSM (Zákány et al., 2001). The functional significance of this observation was uncertain because *Hoxd1* mutant mice had no obvious segmentation alterations in the paraxial mesoderm (Zákány et al., 2001). Interestingly, however, *Hoxd3* mutants have a partial loss of the atlas, which became an almost complete loss when *Hoxa3* was concomitantly inactivated (Condie and Capecchi, 1994). This phenotype is complementary to that observed in both *Dll1-Hoxb6*$^{\Delta LR}$ transgenics and in pH7-Hes7-3 mice. Therefore, *Hoxd3* might regulate the transition from occipital- to cervical-fated somites by fine-tuning *Hes7* oscillations. Further experiments will be required to specifically investigate whether this is the case.

In more posterior areas of the embryo, forced *Hoxb6* expression interfered with the segmentation process in the PSM, possibly through dysregulation of *Lfng* expression. Interestingly, this effect was observed in post-hindlimb but not pre-hindlimb areas of the axis. The differential effect of Hoxb6 on somitogenesis at these two axial levels suggests that the mechanisms of paraxial segmentation are not uniform along the main body axis. Genetic experiments have already revealed that formation of the most anterior 10-12 somites relies on mechanisms that differ from those described for more posterior body areas (Shifley et al., 2008; Williams et al., 2014). Our data now suggest that mechanistic differences might also exist between the formation of somites anterior or posterior to the hindlimb bud. This conclusion fits with previous observations indicating that the segmentation clock may use different regulatory mechanisms at different levels of the anterior-posterior axis. In particular, whereas proper somitogenesis at the thoracic level required *Lfng* oscillatory expression, normal sacral and caudal vertebrae formed in embryos lacking *Lfng* oscillations in the PSM (Shifley et al., 2008). Therefore, the mechanisms regulating somitogenesis might undergo a second switch at the approximate level of the trunk-to-tail transition, which might indicate that it is associated with the transition from epiblast- to tail bud-derived paraxial mesoderm.

Our transgenic experiments show that the PSM tolerates high levels of *Hoxb6* expression within its physiological domain of activity (i.e. the prospective thoracic area) but is less tolerant in the lumbar or sacral regions where *Hoxb6* plays little or no functional role during normal development. Although these experiments involved an overexpression approach, they might still reflect the need for precise regulation of *Hoxb6* spatiotemporal expression. Consistent with this, *Hoxb6* expression is turned down in the PSM at stages when it is producing post-thoracic axial structures. Interestingly, a similar type of downregulation has been described for other Hox genes involved in the patterning of the thoracic domain (Yekta et al., 2008). In the case of *Hoxb8*, and probably also *Hoxa7*, *Hoxc8* and *Hoxd8*, this regulation involves miRs, particularly those of the miR196 family (Yekta et al., 2004, 2008). Whether fine-tuning of *Hoxb6* expression in the PSM is also under miR regulation is not clear. In favor of this hypothesis, the *Hoxb6* 3′UTR contains several potential miR binding sites that are conserved between mouse and human. Particularly interesting are those for miR199, as its inactivation results in malformed vertebrae (Watanabe et al., 2008), and those for the miR196 family because mice lacking all three members of this family have extra lumbar ribs (Wong et al., 2015), resembling the effect of ectopic *Hoxb6* activation. However, removing the binding sites for these two miRs from the *Hoxb6* 3′UTR had no effect on the development of the axial skeleton or on *Hoxb6* expression. Therefore, our experiments failed to confirm the involvement of miR199 and miR196 in the regulation of *Hoxb6* expression in the posterior embryonic axis. Whether this is compensated by other miRs also predicted to bind the *Hoxb6* 3′UTR remains to be determined. In addition, evaluating the importance of *Hoxb6* downregulation in the PSM for proper formation of the post-thoracic skeleton must await the identification of the mechanisms involved in this regulatory process.

Finally, the ability of Hoxb6 to affect anterior-posterior somitic polarity in the PSM is of interest considering that ribs are formed from the posterior somitic compartment (Aoyama and Asamoto, 2000). It is therefore possible that the formation of rib-containing or ribless areas of the skeleton requires the introduction of some type of as yet unidentified anterior posterior pattern in the nascent somite that will later impact the mechanisms of somite differentiation during formation of the axial skeleton.

MATERIALS AND METHODS

Mutant constructs and transgenic mice

Hox PG6 sequences were obtained from the NCBI database and aligned using ClustalW2. All *Hoxb6* constructs were derived from IMAGE clone 4548382, which contains the full-length cDNA of the human gene (*HOXB6*). Mouse *Hoxa7* cDNAs were derived from IMAGE clone 4986801, previously repaired to include the complete open reading frame. All Hox proteins were modified to incorporate a Flag tag at their N-terminus. A similar tag was also present in Pax3 (Guerreiro et al., 2013). Deletion and swapping mutants were produced using a PCR-based mutagenesis strategy (Guerreiro et al., 2012) and their sequences verified.

The transgenic constructs contained the cDNAs downstream of the *msd* enhancer of *Dll1* (Beckers et al., 2000) and upstream of the SV40 polyadenylation signal. *Hoxb6* constructs included either the first 195 bp of the 3′UTR (up to the *Xho*I site) or the whole 3′UTR (686 bp). If not specified, constructs contained the short version of the 3′UTR. Transgenic constructs were released from the plasmid backbone, gel purified and microinjected according to standard procedures (Hogan et al., 1994).

Hoxb6$^{\Delta 3'UTR412\text{-}474}$ mutant mice were generated using CRISPR/Cas9 (Wang et al., 2013). Cas9 mRNA was produced by *in vitro* transcription using the mMESSAGE mMACHINE T7 Ultra Kit (Life Technologies) and plasmid pT7-Cas9 as a template. pT7-Cas9 was constructed by cloning the Cas9 coding region of pX330 (Cong et al., 2013) into pBluescript II KS (Stratagene), downstream of its T7 promoter. sgRNAs were produced by *in vitro* transcription using the MEGAshortscript T7 Kit (Life Technologies). The templates were variants of plasmid pgRNAbasic that included the 20 nucleotide seeding sequences indicated in Fig. 8. pgRNAbasic consisted of the sgRNA coding sequence of pX330 cloned downstream of the T7 promoter. sgRNAs and Cas9 mRNA were purified with the MEGAclear Kit (Life Technologies). Homologous recombination was promoted by a 120 nucleotide single-stranded (ss) DNA oligonucleotide containing the 60 nucleotide sequences on each side of the deletion separated by an *Eco*RI site.

Cas9 mRNA (10 ng/ml), sgRNA1 and sgRNA2 (10 ng/ml each) and the ssDNA oligonucleotide (10 ng/ml) were injected into the pronuclei of fertilized oocytes using standard procedures (Hogan et al.,

1994). Deletions were assessed by PCR from tail genomic DNA using primers 5′-ATGTCTCCTGGAAGCAGAGC-3′ and 5′-TTCACGTCCG-GAGCTAAGAC-3′. The deletion was confirmed by direct sequencing. These primers were also used for genotyping mice and embryos of the *Hoxb6*$^{\Delta 3'UTR412\text{-}474}$ line.

All experiments conducted on animals followed the Portuguese (Portaria 1005/92) and European (Directive 2010/63/EU) legislations concerning housing, husbandry and welfare. The project was reviewed and approved by the Ethics Committee of Instituto Gulbenkian de Ciência and by the Portuguese National Entity Direcção Geral de Alimentação Veterinária (license reference: 014308).

Phenotypic and biochemical analyses

Skeletal phenotypes were analyzed at E18.5 by Alcian Blue/Alizarin Red staining as previously described (Mallo and Brändlin, 1997). Whole-mount *in situ* hybridization (ISH) was performed using DIG-labeled antisense RNA probes as described (Kanzler et al., 1998). ISH experiments typically included three embryos per probe and genotype, with the exception of those involving *Lfng* and *Hes7*, which included at least six embryos. Embryos stained by ISH were embedded in gelatin/albumin and sectioned with a vibratome.

Electrophoretic mobility shift assays were performed as previously described (Guerreiro et al., 2012) using proteins produced in 293T cells. The DNA probe corresponding to the H1 enhancer has been described previously (Guerreiro et al., 2012).

Acknowledgements

We thank Andreas Kispert, Bernhard Herrmann and Achim Gossler for sharing *in situ* probes; Feng Zhang for plasmid pX330; and members of the M.M. laboratory for helpful comments throughout the course of this work.

Competing interests

The authors declare no competing or financial interests.

Author contributions

A.C. performed experiments, contributed to the experimental design and data analysis, and wrote the manuscript. A.N. performed experiments. M.M. conceived and supervised the project, contributed to experimental design and data analysis, and edited the manuscript.

Funding

This work was supported by a grant [PTDC/SAU-BID/110640/2009] to M.M. and by a postdoctoral fellowship [SFRH/BPD/89500/2012] to A.C., both from Fundação para a Ciência e a Tecnologia, Portugal.

Supplementary information

Supplementary information available online at
http://dev.biologists.org/lookup/suppl/doi:10.1242/dev.133074/-/DC1

References

Aoyama, H. and Asamoto, K. (2000). The developmental fate of the rostral/caudal half of a somite for vertebra and rib formation: experimental confirmation of the resegmentation theory using chick-quail chimeras. *Mech. Dev.* **99**, 71-82.

Baker, R. E., Schnell, S. and Maini, P. K. (2006). A clock and wavefront mechanism for somite formation. *Dev. Biol.* **293**, 116-126.

Becker, D., Jiang, Z., Knodler, P., Deinard, A. S., Eid, R., Kidd, K. K., Shashikant, C. S., Ruddle, F. H. and Schughart, K. (1996). Conserved regulatory element involved in the early onset of Hoxb6 gene expression. *Dev. Dyn.* **205**, 73-81.

Beckers, J., Caron, A., de Angelis, M. H., Hans, S., Campos-Ortega, J. A. and Gossler, A. (2000). Distinct regulatory elements direct Delta1 expression in the nervous system and paraxial mesoderm of transgenic mice. *Mech. Dev.* **95**, 23-34.

Brent, A. E. and Tabin, C. J. (2002). Developmental regulation of somite derivatives: muscle, cartilage and tendon. *Curr. Opin. Genet. Dev.* **12**, 548-557.

Bussen, M., Petry, M., Schuster-Gossler, K., Leitges, M., Gossler, A. and Kispert, A. (2004). The T-box transcription factor Tbx18 maintains the separation of anterior and posterior somite compartments. *Genes Dev.* **18**, 1209-1221.

Carapuço, M., Nóvoa, A., Bobola, N. and Mallo, M. (2005). Hox genes specify vertebral types in the presomitic mesoderm. *Genes Dev.* **19**, 2116-2121.

Casaca, A., Santos, A. C. and Mallo, M. (2014). Controlling Hox gene expression and activity to build the vertebrate axial skeleton. *Dev. Dyn.* **243**, 24-36.

Condie, B. G. and Capecchi, M. R. (1994). Mice with targeted disruptions in the paralogous genes hoxa-3 and hoxd-3 reveal synergistic interactions. *Nature* **370**, 304-307.

Cong, L., Ran, F. A., Cox, D., Lin, S., Barretto, R., Habib, N., Hsu, P. D., Wu, X., Jiang, W., Marraffini, L. A. et al. (2013). Multiplex genome engineering using CRISPR/Cas systems. *Science* **339**, 819-823.

Conlon, R., Reaume, A. G. and Rossant, J. (1995). Notch1 is required for the coordinate segmentation of somites. *Development* **121**, 1533-1545.

Dequéant, M.-L., Glynn, E., Gaudenz, K., Wahl, M., Chen, J., Mushegian, A. and Pourquie, O. (2006). A complex oscillating network of signaling genes underlies the mouse segmentation clock. *Science* **314**, 1595-1598.

Duboule, D. (2007). The rise and fall of Hox gene clusters. *Development* **134**, 2549-2560.

Evrard, Y. A., Lun, Y., Aulehla, A., Gan, L. and Johnson, R. L. (1998). Lunatic fringe is an essential mediator of somite segmentation and patterning. *Nature* **394**, 377-381.

Gebelein, B., Culi, J., Ryoo, H. D., Zhang, W. and Mann, R. S. (2002). Specificity of Distalless repression and limb primordia development by abdominal Hox proteins. *Dev. Cell* **3**, 487-498.

Guerreiro, I., Casaca, A., Nunes, A., Monteiro, S., Novoa, A., Ferreira, R. B., Bom, J. and Mallo, M. (2012). Regulatory role for a conserved motif adjacent to the homeodomain of Hox10 proteins. *Development* **139**, 2703-2710.

Guerreiro, I., Nunes, A., Woltering, J. M., Casaca, A., Nóvoa, A., Vinagre, T., Hunter, M. E., Duboule, D. and Mallo, M. (2013). Role of a polymorphism in a Hox/Pax-responsive enhancer in the evolution of the vertebrate spine. *Proc. Natl. Acad. Sci. USA* **110**, 10682-10686.

Harima, Y., Takashima, Y., Ueda, Y., Ohtsuka, T. and Kageyama, R. (2013). Accelerating the tempo of the segmentation clock by reducing the number of introns in the Hes7 gene. *Cell Rep.* **3**, 1-7.

Hogan, B., Beddington, R., Constantini, F. and Lacy, E. (1994). *Manipulating the Mouse Embryo: A Laboratory Manual*. Cold Spring Harbor: Cold Spring Harbor Laboratory Press.

Hubaud, A. and Pourquié, O. (2014). Signalling dynamics in vertebrate segmentation. *Nat. Rev. Mol. Cell Biol.* **15**, 709-721.

In der Rieden, P. M. J., Mainguy, G., Woltering, J. M. and Durston, A. J. (2004). Homeodomain to hexapeptide or PBC-interaction-domain distance: size apparently matters. *Trends Genet.* **20**, 76-79.

Joshi, R., Sun, L. and Mann, R. (2010). Dissecting the functional specificities of two Hox proteins. *Genes Dev.* **24**, 1533-1545.

Kanzler, B., Kuschert, S. J., Liu, Y. H. and Mallo, M. (1998). Hoxa-2 restricts the chondrogenic domain and inhibits bone formation during development of the branchial area. *Development* **125**, 2587-2597.

Mallo, M. and Brändlin, I. (1997). Segmental identity can change independently in the hindbrain and rhombencephalic neural crest. *Dev. Dyn.* **210**, 146-156.

Mallo, M., Vinagre, T. and Carapuço, M. (2009). The road to the vertebral formula. *Int. J. Dev. Biol.* **53**, 1469-1481.

Mallo, M., Wellik, D. M. and Deschamps, J. (2010). Hox genes and regional patterning of the vertebrate body plan. *Dev. Biol.* **344**, 7-15.

Mann, R. S., Lelli, K. M. and Joshi, R. (2009). Hox specificity: unique roles for cofactors and collaborators. *Curr. Top. Dev. Biol.* **88**, 63-101.

McIntyre, D. C., Rakshit, S., Yallowitz, A. R., Loken, L., Jeannotte, L., Capecchi, M. R. and Wellik, D. M. (2007). Hox patterning of the vertebrate rib cage. *Development* **134**, 2981-2989.

Merabet, S., Kambris, Z., Capovilla, M., Bérenger, H., Pradel, J. and Graba, Y. (2003). The hexapeptide and linker regions of the AbdA Hox protein regulate its activating and repressive functions. *Dev. Cell* **4**, 761-768.

Morimoto, M., Takahashi, Y., Endo, M. and Saga, Y. (2005). The Mesp2 transcription factor establishes segmental borders by suppressing Notch activity. *Nature* **435**, 354-359.

Morimoto, M., Sasaki, N., Oginuma, M., Kiso, M., Igarashi, K., Aizaki, K.-I., Kanno, J. and Saga, Y. (2007). The negative regulation of Mesp2 by mouse Ripply2 is required to establish the rostro-caudal patterning within a somite. *Development* **134**, 1561-1569.

Neidhardt, L. M., Kispert, A. and Herrmann, B. G. (1997). A mouse gene of the paired-related homeobox class expressed in the caudal somite compartment and in the developing vertebral column, kidney and nervous system. *Dev. Genes Evol.* **207**, 330-339.

Oginuma, M., Takahashi, Y., Kitajima, S., Kiso, M., Kanno, J., Kimura, A. and Saga, Y. (2010). The oscillation of Notch activation, but not its boundary, is required for somite border formation and rostral-caudal patterning within a somite. *Development* **137**, 1515-1522.

Oka, C., Nakano, T., Wakeham, A., de la Pompa, J. L., Mori, C., Sakai, T., Okazaki, S., Kawaichi, M., Shiota, K., Mak, T. W. et al. (1995). Disruption of the mouse RBP-J kappa gene results in early embryonic death. *Development* **121**, 3291-3301.

Palmeirim, I., Henrique, D., Ish-Horowicz, D. and Pourquié, O. (1997). Avian hairy gene expression identifies a molecular clock linked to vertebrate segmentation and somitogenesis. *Cell* **91**, 639-648.

Papadopoulos, D. K., Reséndez-Pérez, D., Cárdenas-Chávez, D. L., Villanueva-Segura, K., Canales-del-Castillo, R., Felix, D. A., Fünfschilling, R. and

Development (2016) 143, 437-448 doi:10.1242/dev.133074

Gehring, W. J. (2011). Functional synthetic Antennapedia genes and the dual roles of YPWM motif and linker size in transcriptional activation and repression. *Proc. Natl. Acad. Sci. USA* **108**, 11959-11964.
Pearson, J. C., Lemons, D. and McGinnis, W. (2005). Modulating Hox gene functions during animal body patterning. *Nat. Rev. Genet.* **6**, 893-904.
Prince, V. E. (2002). The Hox paradox: more complex(es) than imagined. *Dev. Biol.* **249**, 1-15.
Reed, H. C., Hoare, T., Thomsen, S., Weaver, T. A., White, R. A., Akam, M. and Alonso, C. R. (2010). Alternative splicing modulates Ubx protein function in Drosophila melanogaster. *Genetics* **184**, 745-758.
Saga, Y., Hata, N., Koseki, H. and Taketo, M. M. (1997). Mesp2: a novel mouse gene expressed in the presegmented mesoderm and essential for segmentation initiation. *Genes Dev.* **11**, 1827-1839.
Sharkey, M., Graba, Y. and Scott, M. P. (1997). Hox genes in evolution: protein surfaces and paralog groups. *Trends Genet.* **13**, 145-151.
Shifley, E. T., Vanhorn, K. M., Perez-Balaguer, A., Franklin, J. D., Weinstein, M. and Cole, S. E. (2008). Oscillatory lunatic fringe activity is crucial for segmentation of the anterior but not posterior skeleton. *Development* **135**, 899-908.
Vinagre, T., Moncaut, N., Carapuco, M., Novoa, A., Bom, J. and Mallo, M. (2010). Evidence for a myotomal Hox/Myf cascade governing nonautonomous control of rib specification within global vertebral domains. *Dev. Cell* **18**, 655-661.
Wang, H., Yang, H., Shivalila, C. S., Dawlaty, M. M., Cheng, A. W., Zhang, F. and Jaenisch, R. (2013). One-step generation of mice carrying mutations in multiple genes by CRISPR/Cas-mediated genome engineering. *Cell* **153**, 910-918.
Watanabe, T., Sato, T., Amano, T., Kawamura, Y., Kawamura, N., Kawaguchi, H., Yamashita, N., Kurihara, H. and Nakaoka, T. (2008). Dnm3os, a non-coding RNA, is required for normal growth and skeletal development in mice. *Dev. Dyn.* **237**, 3738-3748.
Wellik, D. M. (2009). Hox genes and vertebrate axial pattern. *Curr. Top. Dev. Biol.* **88**, 257-278.
Wellik, D. M. and Capecchi, M. R. (2003). Hox10 and Hox11 genes are required to globally pattern the mammalian skeleton. *Science* **301**, 363-367.
Williams, D. R., Shifley, E. T., Lather, J. D. and Cole, S. E. (2014). Posterior skeletal development and the segmentation clock period are sensitive to Lfng dosage during somitogenesis. *Dev. Biol.* **388**, 159-169.
Wong, P. C., Zheng, H., Chen, H., Becher, M. W., Sirinathsinghji, D. J. S., Trumbauer, M. E., Chen, H. Y., Price, D. L., Van der Ploeg, L. H. T. and Sisodia, S. S. (1997). Presenilin 1 is required for Notch1 and Dll1 expression in the paraxial mesoderm. *Nature* **387**, 288-292.
Wong, S. F. L., Agarwal, V., Mansfield, J. H., Denans, N., Schwartz, M. G., Prosser, H. M., Pourquié, O., Bartel, D. P., Tabin, C. J. and McGlinn, E. (2015). Independent regulation of vertebral number and vertebral identity by microRNA-196 paralogs. *Proc. Natl. Acad. Sci. USA* **112**, E4884-E4893.
Yekta, S., Shih, I.-H. and Bartel, D. P. (2004). MicroRNA-Directed cleavage of Hoxb8 mRNA. *Science* **304**, 594-596.
Yekta, S., Tabin, C. J. and Bartel, D. P. (2008). MicroRNAs in the Hox network: an apparent link to posterior prevalence. *Nat. Rev. Genet.* **9**, 789-796.
Zákány, J., Kmita, M., Alarcon, P., de la Pompa, J.-L. and Duboule, D. (2001). Localized and transient transcription of Hox genes suggests a link between patterning and the segmentation clock. *Cell* **106**, 207-217.
Zhao, Y. and Potter, S. (2001). Functional specificity of the Hoxa13 homeobox. *Development* **128**, 3197-3207.
Zhao, Y. and Potter, S. S. (2002). Functional comparison of the Hoxa4, Hoxa10 and Hoxa11 homeoboxes. *Dev. Biol.* **244**, 21-36.